Generation of −10.7 dB unbiased entangled states of light

Cite as: Appl. Phys. Lett. **118**, 134001 (2021); https://doi.org/10.1063/5.0041289
Submitted: 21 December 2020 . Accepted: 17 March 2021 . Published Online: 29 March 2021

Yajun Wang, Wenhui Zhang, Ruixin Li, Long Tian, and Yaohui Zheng

Applied Physics Letters ARTICLE scitation.org/journal/apl

Generation of −10.7 dB unbiased entangled states of light

Cite as: Appl. Phys. Lett. **118**, 134001 (2021); doi: 10.1063/5.0041289
Submitted: 21 December 2020 · Accepted: 17 March 2021 ·
Published Online: 29 March 2021

Yajun Wang,[1,2] Wenhui Zhang,[1] Ruixin Li,[1] Long Tian,[1,2] and Yaohui Zheng[1,2,a)]

AFFILIATIONS

[1]State Key Laboratory of Quantum Optics and Quantum Optics Devices, Institute of Opto-Electronics, Shanxi University, Taiyuan 030006, People's Republic of China
[2]Collaborative Innovation Center of Extreme Optics, Shanxi University, Taiyuan 030006, People's Republic of China

Note: This paper is part of the APL Special Collection on Non-Classical Light Emitters and Single-Photon Detectors.
[a)]**Author to whom correspondence should be addressed:** yhzheng@sxu.edu.cn

ABSTRACT

In a continuous variable quantum key distribution (CV-QKD) system, strong Einstein–Podolsky–Rosen entangled states can significantly boost the robustness and distance for secure communication. However, an inevitable bias of two entanglement quadratures may degrade the secret key rate and distance during random quadrature base switching. The bias originates from several interdependent factors in the generation, propagation, and detection of entangled states, which faces a challenge to be completely eliminated. Here, we analyze in detail the origin of the bias effect and report on a scheme of generating unbiased entangled states, whereby a -10.7 ± 0.1 dB quadrature noise unbiased entanglement is first generated experimentally with two single-mode squeezed states. The unbiased quadrature correlations within the measurement bandwidth are expected to immensely enhance the key rate and secure distance for CV-QKD.

Continuous variable (CV) Einstein–Podolsky–Rosen (EPR) entangled states are widely used in quantum key distribution (QKD),[1–5] quantum storage,[6] quantum entanglement swapping,[7–10] quantum computation,[11,12] quantum dense coding,[13,14] and quantum information networks[15–18] due to the quadratures of the two subsystems possessing quantum correlations. Therein, CV-QKD systems are encoded in the quadratures of the quantized electromagnetic field, such as those of coherent states, and homodyne or heterodyne detection techniques are used for signal extraction.[2,19,20] It promises information theoretic security in data communication and is currently being prepared for commercial applications. However, before QKD can be widely popularized in real-life, it is confronted with a number of main challenges,[3,21] i.e., secret key rate, distance, speed, size, cost, and practical security.[19,22–26]

To enlarge the secret key rate and distance, one obvious strategy is to reduce the channel loss and excess noise and to increase the post-processing efficiency. Recently, the maximum security distance was already reached at 202 km fiber for the coherent-based protocol by combining a phase compensation and highly efficient post-processing techniques,[27] which represented a more practical way for the implementation of the CV-QKD. This also highlights a limitation of existing repeaterless QKD schemes—they can never surpass the secret key capacity (SKC) bound [or Pirandola–Laurenza–Ottaviani–Banchi (PLOB) bound].[28,29] Theoretical and experimental evidence demonstrated that a CV-QKD protocol based on entangled states can be more tolerant to channel excess noise, loss, and limited post-processing efficiency.[3–5,19,30] For instance, using a −3.5 dB of impure and modulated two-mode squeezing, a secret raw key was generated between two parties connected by a noisy and lossy channel, a channel that is not secure for coherent state protocols, which significantly boost the robustness and distance for secure communication.[3] Nevertheless, the communication distance and secret key rate are directly related to the magnitude of the quantum correlations of the quadratures for entangled states.[30] If two users, Alice and Bob, share a long random string of secret bits—the key—then they can achieve secure communication by encrypting their messages with the standard one-time-pad encryption scheme. During the decryption, they also randomly extract the information based on a random quadrature base. Therefore, in order to keep the advantages of the entangled source in a long distance and high secret key rate for CV-QKD communication, the entangled states should be prepared not only with strong quantum correlations[22,23] but also with unbiased quantum correlations[24] to satisfy the measurement for random quadrature bases.

For a variety of EPR applications, researchers have realized the significance of symmetric entanglement.[3,24,25,31] In a practical

quantum system, the bias effect is inevitable, especially for high degree EPR generation,[22] unless there is an active manipulation. The bias originates from several interdependent factors in the generation, propagation, and detection of entangled states, which faces challenge to be completely eliminated. Currently, CV-QKD based on EPR quantum correlation has been experimentally or theoretically demonstrated without considering the influence of the bias effect between the two quadrature components.[3,4,25,30] This inspired a subsequent work, which exploited a method to complete two key challenge indicators for EPR entanglement: (1) generation of high entanglement degree for the two quadrature components; and (2) achievement of an unbiased entanglement under premise of keeping a high entanglement degree. In comparison with the physical properties of unidimensional and two dimensional protocols in coherent or squeezed states, the bias effect will contravene the random quadrature base measurement rule and may weaken the secure distance for CV-QKD due to some information discarding in one of the measured quadratures.[3,32–38]

This work completely quantifies the study of the bias effect in EPR state preparation and allows us to build controllable quantum correlations with the experimental parameters, i.e., channel losses, squeezing factors, and ratio of the beam splitter. An unbiased entanglement with −10.7 dB@5 MHz below the quantum noise limit (QNL) was experimentally established. Meanwhile, the unbiased correlations also showed a significant performance in a broadband frequency spectrum within the bandwidth of the squeezer.

An entanglement state is generally prepared by coupling two equivalent squeezed states, i.e., $V_a = V_b$. In a realistic scenario, several parameters may destroy the symmetric correlations and introduce a bias effect.[24,31] Therefore, the EPR correlations should be globally reconsidered under a non-ideal condition. By introducing the losses in the optical channel of the EPR modes (ε_a and ε_b) and balance of the 50/50 BS ((1-T):T), the amplitude and phase quadrature variances of the two modes of the EPR states are deduced as

$$V_a(X) = \left[TV_2(Y) + (1-T)V_1(X)\right](1-\varepsilon_a) + \varepsilon_a, \quad (1)$$

$$V_a(Y) = \left[TV_2(X) + (1-T)V_1(Y)\right](1-\varepsilon_a) + \varepsilon_a, \quad (2)$$

$$V_b(X) = \left[(1-T)V_2(Y) + TV_1(X)\right](1-\varepsilon_b) + \varepsilon_b, \quad (3)$$

$$V_b(Y) = \left[(1-T)V_2(X) + TV_1(Y)\right](1-\varepsilon_b) + \varepsilon_b. \quad (4)$$

Based on the theory in Refs. 38 and 39, the quantum correlation variances for the two quadratures can be inferred as

$$V\left(\hat{X}_a + \hat{X}_b\right) = \alpha_1 V_1(X) + \beta_1 V_2(Y) + \varepsilon_a + \varepsilon_b, \quad (5)$$

$$V\left(\hat{Y}_a - \hat{Y}_b\right) = \alpha_2 V_1(Y) + \beta_2 V_2(X) + \varepsilon_a + \varepsilon_b, \quad (6)$$

where $\hat{X}_{a,b}$ ($\hat{Y}_{a,b}$) is the amplitude (phase) quadrature operator. $\alpha_1, \alpha_2, \beta_1$, and β_2 are the noise coupling coefficients:

$$\alpha_1 = (1-\varepsilon_a)(1-T) + (1-\varepsilon_b)T + 2\sqrt{(1-\varepsilon_a)(1-\varepsilon_b)}\sqrt{T}\sqrt{1-T}, \quad (7)$$

$$\beta_1 = (1-\varepsilon_a)T + (1-\varepsilon_b)(1-T) - 2\sqrt{(1-\varepsilon_a)(1-\varepsilon_b)}\sqrt{T}\sqrt{1-T}, \quad (8)$$

$$\alpha_2 = (1-\varepsilon_a)(1-T) + (1-\varepsilon_b)T - 2\sqrt{(1-\varepsilon_a)(1-\varepsilon_b)}\sqrt{T}\sqrt{1-T}, \quad (9)$$

$$\beta_2 = (1-\varepsilon_a)T + (1-\varepsilon_b)(1-T) + 2\sqrt{(1-\varepsilon_a)(1-\varepsilon_b)}\sqrt{T}\sqrt{1-T}, \quad (10)$$

where $V_1(Y), V_2(Y)$ are the phase (anti-squeezing in our scenario) quadrature variances of the two squeezed states.[22,40,41] Apparently, the deviation of the three parameters ($V_{1,2}(X)$, T, $\varepsilon_{a,b}$) will introduce a bias effect $\Delta V = V(\hat{X}_a + \hat{X}_b) - V(\hat{Y}_a - \hat{Y}_b)$ for the two quadrature correlations, which should be comprehensively interpreted.

Typically, with $\varepsilon_{a,b} = 0$ and $T = 0.5$, then $\alpha_1 = \beta_2 = 2$ and $\beta_1 = \alpha_2 = 0$, and the quantum correlations are simplified to $V(\hat{X}_a + \hat{X}_b) = 2V_1(X)$ and $V(\hat{Y}_a - \hat{Y}_b) = 2V_2(X)$, in which the influence of the anti-squeezing quadrature is vanished. If an unbiased entanglement is demanded, the identical variance for the two squeezing must be fabricated to meet the requirement.

Second, for the case of $T = 0.5$ or $\varepsilon_a = \varepsilon_b$, the transformation coefficients are reduced to $\alpha_1 = \beta_2$ and $\beta_1 = \alpha_2$, that is to say, an unbiased entanglement can be also produced under the condition of $V_1(X) = V_2(X)$.

Third, for a small bias of $\varepsilon_{a,b}$ and T, a biased entanglement is produced, which is mainly attributed to the different noise coupling in the amplitude ($\alpha_1 V_1(X)$) and phase squeezing ($\beta_2 V_2(X)$) ($\alpha_1 \neq \beta_2 \approx 2$) and partly attributed to that of the anti-squeezing components ($\beta_1 V_2(Y), \alpha_2 V_1(Y), \beta_1 \neq \alpha_2 \approx 0$). It can be found that $\alpha_1 V_1(X)$ has a major contribution to the amplitude correlation, and the phase correlation is sensitive to $\beta_2 V_2(X)$.

The channel losses $\varepsilon_{a,b}$ are first confirmed as constant. The EPR quantum correlations are manipulated by T or $V_2(X)$. (1) Fig. 1(a): a −11 dB amplitude squeezing is coupled with the other squeezing by an unbalanced BS ($T = 0.485$) and different optical losses ($\varepsilon_a = 0.03, \varepsilon_b = 0.01$). When $V_2(X) = -10.5$ dB, an unbiased entanglement is produced as −9.5 dB. (2) Figure 1(b): with the same loss as (a) and $V_1(X) = V_2(X) = -11$ dB, but T is identified as the independent variable. An unbiased entangled state (−10 dB) appears at $T = 0.5$. Figs. 1(a) and 1(b) demonstrate that the noise variances of the two quadratures will exchange magnitude at the symmetrical sides of the unbiased point. Compared with the two methods [Figs. 1(a) and 1(b)], the balance of the BS will produce the highest degree of EPR entanglement.

Subsequently, ε_a is constant and ε_b simulates a real loss environment. The results are shown in Fig. 1(c): the amplitude correlation is insensitive to the optical loss ε_b, which induces a larger ΔV after the point of the intersection with the loss increasing. It is due to the effect that the noise coupling of ε_b in α_1 ($T = 0.485$) is smaller than that in β_2 ($1 - T = 0.515$), which will import less noise to the amplitude sum correlation than the phase difference one.

In a word, when the squeezing factors from the two squeezers are equal, the unbiased entangled states can be prepared by a balanced BS or loss, unnecessary to simultaneously meet the two requirements. However, the optical loss in the quantum channel is uncontrollable in a practical CV-QKD; thus, the balanced BS is more practical. As a result, the unbalanced channel loss ($\varepsilon_a \neq \varepsilon_b$) does not influence the unbiased character for the two quadratures anymore, which is extremely valuable for a CV-QKD based on unbiased entangled states. Figure 2 shows a theoretical relation between the ΔV and secret key rate based on the parameters in Table I, Figs. 1(b) and 1(c), and an EPR CV-QKD protocol in Ref. 4. Secret key rates for three distribution distances (50, 100, and 150 km) are calculated. The results

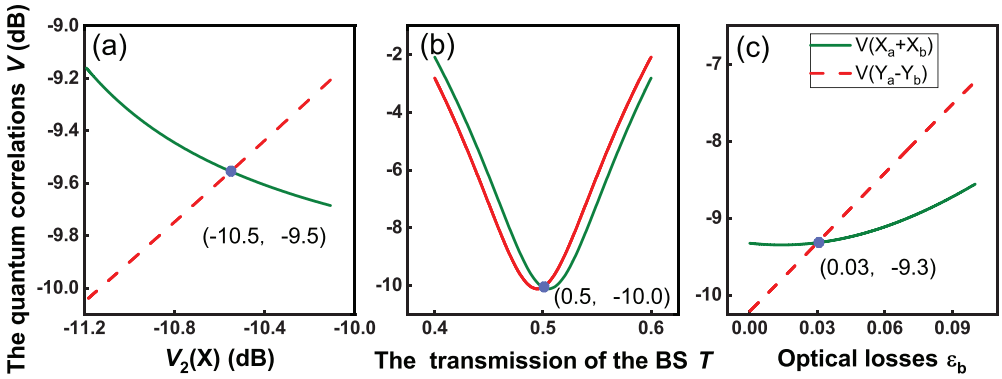

FIG. 1. Theoretical comparison between the quantum correlation variance $V(\hat{X}_a + \hat{X}_b)$ (black solid line) and $V(\hat{Y}_a - \hat{Y}_b)$ (red dashed line) for different $V_{1,2}(X)$, $\varepsilon_{a,b}$, and T (a-c). (a) $T = 0.485, \varepsilon_a = 0.03 \neq \varepsilon_b = 0.01$, and $V_1(X) = -11$ dB; (b) $\varepsilon_a = 0.03 \neq \varepsilon_b = 0.01$ and $V_1(X) = V_2(X) = -11$ dB; and (c) $T = 0.485, \varepsilon_a = 0.03$ and $V_1(X) = V_2(X) = -11$ dB.

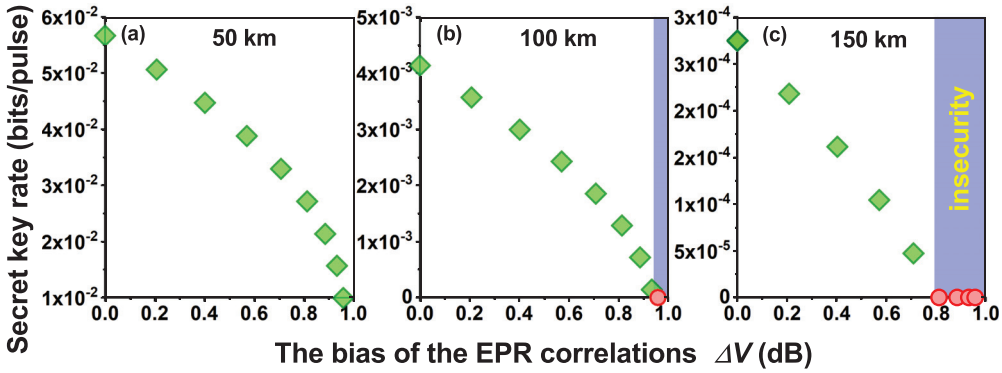

FIG. 2. Secret key rates for three secure distances of 50 km (a), 100 km (b), and 150 km (c) vs the bias correlations ΔV of the entanglement. The circular dots in Figs. 2(b) and 2(c) represent that CV-QKD is insecure for $\Delta I = 0$.

demonstrate that the secret key rate decreases with the increase in ΔV; meanwhile, a larger bias ΔV could result in a shorter maximum secure distance, i.e., a 1 dB biased variance will limit the maximum secure distance to 100 km [Fig. 2(b)].

The experimental schematic diagram of the entangled states generator is shown in Fig. 3. A CV single-frequency fiber laser with 2 W output power (E15, NKT Photonics) is used for the preparation (DOPA) and demodulation (BHD) of the EPR states. The mode cleaners (1550 nm MC1 and MC2) are employed to prepare the local oscillator (LO) for the two BHDs and the seed beams of the two DOPAs (40 mW) and the injection (1.57 W) of the second harmonic generator (SHG) (775 nm-1.12 W). Both of the DOPAs are semi-monolithic singly resonant standing wave cavities with similar parameters in Refs. 18 and 34, except for an air gap of 21 mm and a concave

TABLE I. The parameters used to calculate the secret key rate of Figs. 2(a)–2(c). Note: Refs. 1–5 and 42: the secret key rate of reverse reconciliation (RR): $\Delta I = \beta I_{AB} - \chi_{BE}$, I_{AB} is the Shannon mutual information between the measurement results of Alice and Bob and χ_{BE} represents the Holevo quantity between Bob's data and Eve's quantum states. The QKD protocol is secure, while the key rate $\Delta I > 0$. In biased and unbiased EPR protocols, the purification of the source quantum states is carried out for estimating the key rate. The channel loss is determined by the length of the fiber and is the same as the biased and unbiased protocol for a certain distance. The excess noise is attributed to the phase fluctuations and imperfections in the state's preparation, modulation, transmission, and detection processes.[4,43] The reconciliation efficiency β is a function of the signal-to-noise ratio (SNR) and is also related to the algorithm being used for the reconciliation and computational power in trusted devices. Here, the optimum efficiency for experimental conditions is considered.[42] The details of the strict demonstration will be investigated in a further paper [Zhang *et al.* (unpublished)].

Reconciliation efficiency	Excess noise	Loss coefficient of a fiber	Detection efficiency of Alice	Detection efficiency of Bob	Electronic noise of Bob
β	E	α (dB/km)	η_A	η_B	ν_{elB}
0.99	0.1	0.2	0.99	0.843	0.01

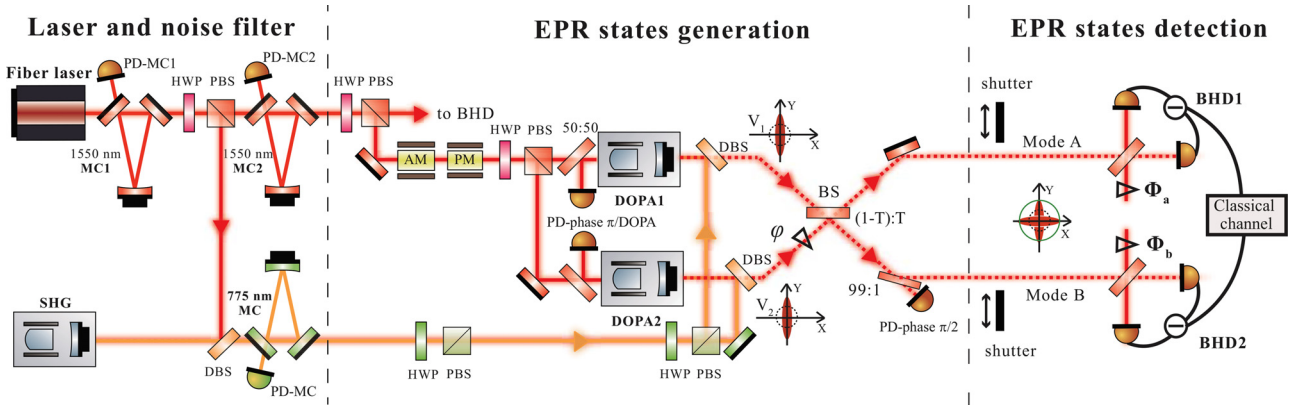

FIG. 3. The schematic of the EPR entangled states. The EPR source, which contains the laser and noise filter, EPR entangled state, and quantum channel of EPR1 and BHD1, is attributable to Alice. AM, amplitude modulator; PM, phase modulator; PBS, polarization beam splitter; SHG, second harmonic generator; MC, mode cleaner; DOPA, degenerate optical parametric amplifier; DBS, dichroic beam splitter; BS, 50/50 beam splitter; PD, photodetector; HWP, half wave plate; BHD, balanced homodyne detector; and Shutter, used to open or close the power attenuation plate.

mirror with a 25 mm radius of curvature. Both DOPAs have a similar finesse (linewidth) of the fundamental wave about 47.2 (83.2 MHz), the escape efficiency about 98.4%, and threshold pump power about 520 mW.

The entangled states are prepared by actively locking the relative phase φ between two squeezing beams to $\pi/2$ with a weak signal from a 99:1 BS. A rotating platform is installed under the BS to adjust the transmissivity T. A power attenuation shutter is applied for loss

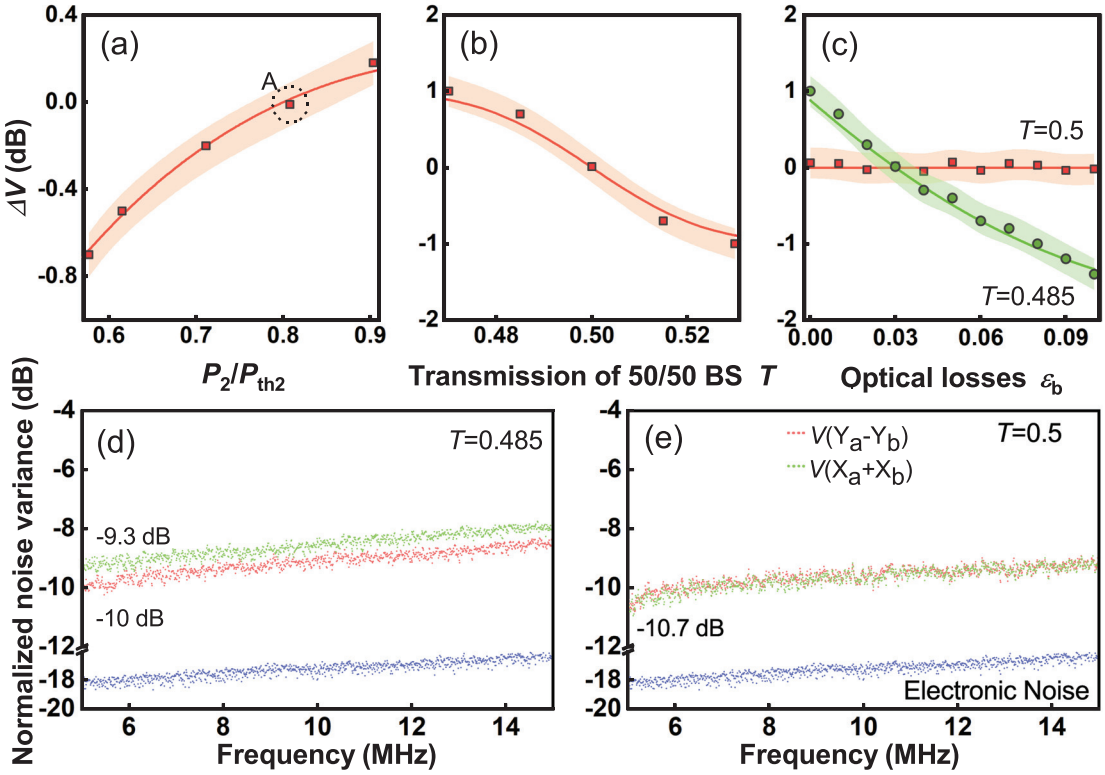

FIG. 4. (a)–(c) Experimental measurement for the dependence of the noise variance asymmetric ΔV on the pump power P_2 of the DOPA2, the transmission T of the BS, and the optical losses ε_a and ε_b. (d) and (e) Noise variances $V(\hat{X}_a + \hat{X}_b)$ and $V(\hat{Y}_a - \hat{Y}_b)$ for the biased and unbiased EPR entangled states. (a) $T = 0.5, \varepsilon_a = 0.03 \neq \varepsilon_b = 0.01$, and $P_1/P_{th1} = 0.8$; (b) $V_1(X) = V_2(X) = -11$ dB and $\varepsilon_a = 0.03 \neq \varepsilon_b = 0.01$; (c) $V_1(X) = V_2(X) = -11$ dB and $\varepsilon_a = 0.03$. (d) $T = 0.485, \varepsilon_a = 0.03 \neq \varepsilon_b = 0.01$, and $P_1/P_{th1} = P_2/P_{th2} = 0.8$, $V(Y_a - Y_b) = -10$ dB and $V(X_a + X_b) = -9.3$ dB@5 MHz; (e) $T = 0.5, \varepsilon_a = 0 \neq \varepsilon_b = 0.01$, and $P_1/P_{th1} = P_2/P_{th2} = 0.8$, $V(X_a + X_b) = V(Y_a - Y_b) = -10.7$ dB@5 MHz. Analysis frequency: 5 MHz, RBW: 300 kHz, and VBW: 100 Hz.

controlling; third, the squeezing and anti-squeezing factors are fine-tuned by the pump power injected into the DOPAs.

It is well known that optical losses reduce the squeezing by mixing vacuum noise into the squeezed quadrature and the phase fluctuations further deteriorate the measured squeezing level by projecting the noise of anti-squeezed quadrature onto the squeezed one. By carefully managing the losses and phase fluctuations, we had generated squeezed states with high squeezing factors,[40,44,45] which is a building block for constructing a 10 dB entangled state. The prerequisite for unbiased entangled state generation is that all the resonators and relative phases in Fig. 3 for the preparation of squeezing and entanglement should be accurately locked as much as possible, whereas a biased effect will appear. For instance, supposing a pair of 11 dB squeezed states is used for entanglement generation, only a phase drift of 12 mrad between the two squeezing modes, neglecting other interfering factors, results in a bias quadrature noise of 1 dB.

To satisfy the requirement of ultralow phase drift for unbiased entanglement generation, some more strict technical conditions have to be developed. Our phase locking technology begins with an amplitude modulator (AM, a modulation frequency of 30 MHz) and/or a phase modulator (PM, a modulation frequency of 40 MHz), and they print a pair of modulation sidebands symmetrical to the carrier frequency of the seed beams injected into the DOPAs. The amplitude modulation signal is demodulated by the downstream photo detector (PD-phase $\pi/2$) for $\pi/2$ phase locking, e.g., the relative phase between the two squeezed modes; the phase modulation signal is extracted by PD-phase π for locking the length of DOPAs with PDH technique or the relative phase of π between the pump and seed beams before DOPA. The modulation signal provides an AC locking technique, which can drastically decrease the zero point drift for the reference point of the phase locking error signal. The DOPA is a highly undercoupled resonator, which makes its output power very low, about 10^{-4} of the seed beam. Therefore, the weak beam brings into a big challenge for the downstream phase locking. To obtain a stable phase locking in the weak signal condition, several improvements have been proposed in our control loop. At first, a high-gain feedback loop is required to reduce the phase fluctuation. Here, we employ a high-Q resonant photodetector (RPD) as the first sensor stage of the feedback loop to improve the signal-to-noise ratio of the error signal.[46,47] Second, the feedback loop should have little zero baseline drift. We design an electro-optic modulator (EOM) with low residual amplitude modulation (RAM) to reduce the relative phase variation with time.[47,48] As two key elements of the feedback loop, both the RPD and low-RAM EOM underpin the low phase fluctuation. Due to the fact that squeezing is sensitive to the phase fluctuations, the fluctuation can be accurately quantified by fitting the relations between the pump power and squeezing variances with the models in Refs. 34–37. As a result, the relative phase φ fluctuation after active control is demonstrated to be only 3.1 mrad, corresponding to 0.06 dB bias quadrature noise (entanglement degree of 11 dB). It is the indispensable prerequisite for constructing unbiased EPR correlations and excludes the phase fluctuations contributing to the bias effect.

During the EPR preparation, the bias effect is studied in detail, by manipulating one of the squeezed states $V_2(X)$, the transmissivity T of the 50/50 BS, and channel losses ε_b. Throughout the experiment, DOPA1 generates a maximum squeezing with a factor of −11 dB, corresponding to an anti-squeezing of 21 dB. Figure 4 shows the bias effect experimentally in two cases. (1) Case I [Figs. 4(a) and 4(c)]: $T = 0.5$, the pump power of DOPA2 is changed to control the squeezing strength, and the shutter in the optical channel of mode A or B is used to manipulate the loss. When the two amplitude squeezed states are with an identical squeezing level, an unbiased entanglement [point A in Fig. 4(a)] is produced. The symmetrical quadrature correlation status is independent of the channel loss [square point in Fig. 4(c)], whereas a biased entanglement is generated [Fig. 4(a)]. (2) Case II [Figs. 4(b) and 4(c)]: $V_1(X) = V_2(X)$, the transmissivity T is changed by tuning the incident angle of the BS. A bigger deviation of the BS from 50:50 results in a larger noise asymmetry ΔV between the two quadrature correlations [Fig. 4(b)]. For a certain splitter ratio $T = 0.485$, ΔV increases with the loss bias growing up [circular dots in Fig. 4(c)], and only when $\varepsilon_b = \varepsilon_a$, an unbiased entanglement is produced. All the measured results are in good agreement with the theoretical ones [the fitted curves in Figs. 4(a)–4(c)].

Figures 4(d) and 4(e) show the broadband noise spectrum for biased and unbiased entangled states with the maximum noise reduction (−10.7 dB, with an inseparability criterion of the correlations $\sqrt{V(\hat{X}_a + \hat{X}_b)V(\hat{Y}_a - \hat{Y}_b)} = 0.085$, is mainly limited by the total optical loss in the system.), which exhibit a frequency independent bias effect, i.e., the biased or unbiased correlations keeps its own noise growing trend, without exchanges identity each other. Here, only the 5–15 MHz broadband noise spectrum is shown, while the higher frequency noise spectrum is omitted, and due to a limited linewidth of the DOPA, the noise reduction rapidly decreases above 15 MHz. Meanwhile, the correlations of the

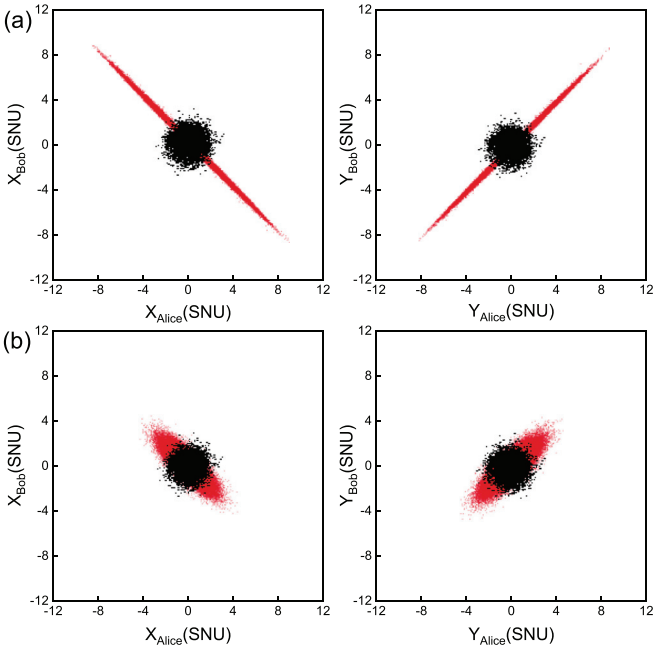

FIG. 5. The measured amplitude X and phase Y quadrature correlations between the two balanced homodyne detectors. The black area represents the coherent state, and the red area is the correlations of the entangled states. (a) Correlations of the initial EPR source without additional channel losses. (b) Correlations with mode B of the EPR source introducing a 90% loss.

amplitude X and phase Y quadrature for unbiased entangled states were measured at the sideband frequency of 5 MHz [Fig. 5(a)], which also presents symmetrical correlations for the two quadratures. Furthermore, a 90% loss was introduced into the optical path of mode B, and then the two quadratures also show symmetrical correlations. The broadband frequency and loss independent unbiased quadrature correlations are expected to immensely enhance the key rate and security distance for CV-QKD.

In conclusion, we theoretically analyze the biased effect in the preparation of entangled states and experimentally demonstrate unbiased entangled states. By optimizing the parameters in the state preparation, transmission, and detection processes, an unbiased entangled state with −10.7 dB @ 5 MHz quadrature correlations was first completed. The results verified a frequency and loss independent unbiased correlation character, which is suitable for the application of high speed and long distance CV-QKD. In the future, the unbiased entanglement source will be expected to apply to a practical available technology and feasible CV-QKD protocol to further boost the secret key rate and distance.

AUTHORS' CONTRIBUTIONS

Y.W. and W.Z. contributed equally to this work.

The authors acknowledge financial support from the National Natural Science Foundation of China (NSFC) (Nos. 62027821, 11654002, 11874250, and 11804207); National Key Research and Development Program of China (No. 2020YFC2200402); Key Research and Development (R&D) Projects of Shanxi Province (No. 201903D111001); Program for Sanjin Scholar of Shanxi Province; Program for Outstanding Innovative Teams of Higher Learning Institutions of Shanxi; and Fund for Shanxi "1331 Project" Key Subjects Construction.

DATA AVAILABILITY

The data that support the findings of this study are available from the corresponding author upon reasonable request.

REFERENCES

[1]T. C. Ralph and P. K. Lam, "A bright future for quantum communications," Nat. Photonics **3**, 671 (2009).
[2]C. Weedbrook, "Continuous-variable quantum key distribution with entanglement in the middle," Phys. Rev. A **87**, 022308 (2013).
[3]L. S. Madsen, V. C. Usenko, M. Lassen, R. Filip, and U. L. Andersen, "Continuous variable quantum key distribution with modulated entangled states," Nat. Commun. **3**, 1083 (2012).
[4]N. Wang, S. N. Du, W. Y. Liu, X. Y. Wang, Y. M. Li, and K. C. Peng, "Long-distance continuous-variable quantum key distribution with entangled states," Phys. Rev. Appl. **10**, 064028 (2018).
[5]N. Wang, S. N. Du, W. Y. Liu, X. Y. Wang, and Y. M. Li, "Generation of Gaussian-modulated entangled states for continuous variable quantum communication," Opt. Lett. **44**, 3613–3616 (2019).
[6]Z. H. Yan, L. Wu, X. J. Jia, Y. H. Liu, R. J. Deng, S. J. Li, H. Wang, C. D. Xie, and K. C. Peng, "Establishing and storing of deterministic quantum entanglement among three distant atomic ensembles," Nat. Commun. **8**, 718 (2017).
[7]S. Takeda, M. Fuwa, P. van Loock, and A. Furusawa, "Entanglement swapping between discrete and continuous variables," Phys. Rev. Lett. **114**, 100501 (2015).
[8]X. J. Jia, X. L. Su, Q. Pan, J. R. Gao, C. D. Xie, and K. C. Peng, "Experimental demonstration of unconditional entanglement swapping for continuous variables," Phys. Rev. Lett. **93**, 250503 (2004).
[9]M. H. Zhang and H. F. Li, "Weak blind quantum signature protocol based on entanglement swapping," Photonics Res. **3**, 324–328 (2015).
[10]X. L. Su, C. X. Tian, X. W. Deng, Q. Li, C. D. Xie, and K. C. Peng, "Quantum entanglement swapping between two multipartite entangled states," Phys. Rev. Lett. **117**, 240503 (2016).
[11]N. C. Menicucci, P. V. Loock, M. Gu, C. Weedbrook, T. C. Ralph, and M. A. Nielsen, "Universal quantum computation with continuous-variable cluster states," Phys. Rev. Lett. **97**, 110501 (2006).
[12]S. H. Lie and H. Jeong, "Limitations of teleporting a qubit via a two-mode squeezed state," Photonics Res. **7**, A7–A13 (2019).
[13]C. X. Cai, L. Ma, J. Li, H. Guo, K. Liu, H. X. Sun, R. G. Yang, and J. R. Gao, "Generation of a continuous-variable quadripartite cluster state multiplexed in the spatial domain," Photonics Res. **6**, 479–484 (2018).
[14]X. Y. Li, Q. Pan, J. T. Jing, J. Zhang, C. D. Xie, and K. C. Peng, "Quantum dense coding exploiting a bright Einstein-Podolsky-Rosen beam," Phys. Rev. Lett. **88**, 047904 (2002).
[15]U. L. Andersen, J. S. Neergaard-Nielsen, P. V. Loock, and A. Furusawa, "Hybrid discrete-and continuous-variable quantum information," Nat. Phys. **11**, 713 (2015).
[16]X. J. Jia, Z. H. Yan, Z. Y. Duan, X. L. Su, H. Wang, C. D. Xie, and K. C. Peng, "Experimental realization of three-color entanglement at optical fiber communication and atomic storage wavelengths," Phys. Rev. Lett. **109**, 253604 (2012).
[17]B. K. Park, M. K. Woo, Y. S. Kim, Y. W. Cho, S. Moon, and S. W. Han, "User-independent optical path length compensation scheme with sub-nanosecond timing resolution for a 1 N quantum key distribution network system," Photonics Res. **8**, 296–302 (2020).
[18]S. Shi, L. Tian, Y. Wang, Y. Zheng, C. Xie, and K. Peng, "Demonstration of channel multiplexing quantum communication exploiting entangled sideband modes," Phys. Rev. Lett. **125**, 070502 (2020).
[19]P. Jouguet, S. Kunz-Jacques, A. Leverrier, P. Grangier, and E. Diamanti, "Experimental demonstration of long-distance continuous-variable quantum key distribution," Nat. Photonics **7**, 378 (2013).
[20]H. Ko, B. S. Choi, J. S. Choe, K. J. Kim, J. H. Kim, and C. J. Youn, "High-speed and high-performance polarization-based quantum key distribution system without side channel effects caused by multiple lasers," Photonics Res. **6**, 214–219 (2018).
[21]G. Zhang, J. Y. Haw, H. Cai, F. Xu, S. M. Assad, J. F. Fitzsimons, Y. Zhang, S. Yu, J. Wu, W. Ser, L. C. Kwek, and A. Q. Liu, "An integrated silicon photonic chip platform for continuous-variable quantum key distribution," Nat. Photonics **13**, 839–842 (2019).
[22]T. Eberle, V. Händchen, and R. Schnabel, "Stable control of 10 dB two-mode squeezed vacuum states of light," Opt. Express **21**, 11546–11553 (2013).
[23]S. Steinlechner, J. Bauchrowitz, T. Eberle, and R. Schnabel, "Strong Einstein-Podolsky-Rosen steering with unconditional entangled states," Phys. Rev. A **87**, 022104 (2013).
[24]W. P. Bowen, P. K. Lam, and T. C. Ralph, "Biased EPR entanglement and its application to teleportation," J. Mod. Opt. **50**, 801–813 (2003).
[25]A. Becir and M. R. B. Wahiddin, "Tight bounds for the eavesdropping collective attacks on general CV-QKD protocols that involve non-maximally entanglement," Quantum Inf. Process. **12**, 1155–1171 (2013).
[26]C. Zhou, X. Y. Wang, Y. C. Zhang, Z. G. Zhang, S. Yu, and H. Guo, "Continuous-Variable Quantum key Distribution with Rateless Reconciliation Protocol," Phys. Rev. Appl. **12**, 054013 (2019).
[27]Y. C. Zhang, Z. Y. Chen, S. Pirandola, X. Y. Wang, C. Zhou, B. J. Chu, Y. J. Zhao, B. J. Xu, S. Yu, and H. Guo, "Long-distance continuous-variable quantum key distribution over 202.81 km of fiber," Phys. Rev. Lett. **125**, 010502 (2020).
[28]S. Pirandola, R. Laurenza, C. Ottaviani, and L. Banchi, "Fundamental limits of repeaterless quantum communications," Nat. Commun. **8**, 15043 (2017).
[29]M. Lucamarini, Z. L. Yuan, J. F. Dynes, and A. J. Shields, "Overcoming the rate–distance limit of quantum key distribution without quantum repeaters," Nature **557**, 400–403 (2018).
[30]V. C. Usenko and R. Filip, "Squeezed-state quantum key distribution upon imperfect reconciliation," New J. Phys. **13**, 113007 (2011).
[31]K. Wagner, J. Janousek, S. Armstrong, J. F. Morizur, P. K. Lam, and H. A. Bachor, "Asymmetric EPR entanglement in continuous variable systems," J. Phys. B **47**, 225502 (2014).

[32]X. Y. Wang, S. Y. Guo, P. Wang, W. Y. Liu, and Y. M. Li, "Realistic rate–distance limit of continuous-variable quantum key distribution," Opt. Express **27**, 13372–13386 (2019).
[33]N. J. Cerf, M. Lévy, and G. V. Assche, "Quantum distribution of Gaussian keys using squeezed states," Phys. Rev. A **63**, 052311 (2001).
[34]V. C. Usenko, "Unidimensional continuous-variable quantum key distribution using squeezed states," Phys. Rev. A **98**, 032321 (2018).
[35]X. Y. Wang, Y. X. Cao, P. Wang, and Y. M. Li, "Advantages of the coherent state compared with squeezed state in unidimensional continuous variable quantum key distribution," Quantum Inf. Process. **17**, 344 (2018).
[36]R. García-Patrón and N. J. Cerf, "Continuous-variable quantum key distribution protocols over noisy channels," Phys. Rev. Lett. **102**, 130501 (2009).
[37]T. Eberle, V. Händchen, J. Duhme, T. Franz, F. Furrer, R. Schnabel, and R. F. Werner, "Gaussian entanglement for quantum key distribution from a single-mode squeezing source," New J. Phys. **15**, 053049 (2013).
[38]T. Eberle, V. Händchen, J. Duhme, T. Franz, R. F. Werner, and R. Schnabel, "Strong Einstein-Podolsky-Rosen entanglement from a single squeezed light source," Phys. Rev. A **83**, 052329 (2011).
[39]J. R. Wang, W. H. Zhang, L. Tian, Y. Wang, R. C. Yang, J. Su, and Y. H. Zheng, "Balanced homodyne detector with independent phase control and noise detection branches," IEEE Access **7**, 57054–57059 (2019).
[40]W. H. Yang, S. P. Shi, Y. J. Wang, W. G. Ma, Y. H. Zheng, and K. C. Peng, "Detection of stably bright squeezed light with the quantum noise reduction of 12.6 dB by mutually compensating the phase fluctuations," Opt. Lett. **42**, 4553–4556 (2017).
[41]H. Vahlbruch, M. Mehmet, K. Danzmann, and R. Schnabel, "Detection of 15 dB squeezed states of light and their application for the absolute calibration of photoelectric quantum efficiency," Phys. Rev. Lett. **117**, 110801 (2016).
[42]M. Milicevic, C. Feng, L. M. Zhang, and P. G. Gulak, "Quasi-cyclic multi-edge LDPC codes for long-distance quantum cryptography," npj Quant. Inf. **4**, 21 (2018).
[43]J. Lodewyck, T. Debuisschert, R. Tualle-Brouri, and P. Grangier, "Controlling excess noise in fiber-optics continuous-variable quantum key distribution," Phys. Rev. A **72**, 050303 (2005).
[44]S. P. Shi, Y. J. Wang, W. H. Yang, Y. H. Zheng, and K. C. Peng, "Detection and perfect fitting of 13.2 dB squeezed vacuum states by considering green-light-induced infrared absorption," Opt. Lett. **43**, 5411–5414 (2018).
[45]W. H. Zhang, J. R. Wang, Y. H. Zheng, Y. J. Wang, and K. C. Peng, "Optimization of the squeezing factor by temperature-dependent phase shift compensation in a doubly resonant optical parametric oscillator," Appl. Phys. Lett. **115**, 171103 (2019).
[46]C. Y. Chen, Z. X. Li, X. L. Jin, and Y. H. Zheng, "Resonant photodetector for cavity-and phase-locking of squeezed state generation," Rev. Sci. Instrum. **87**, 103114 (2016).
[47]Z. X. Li, W. G. Ma, W. H. Yang, Y. J. Wang, and Y. H. Zheng, "Reduction of zero baseline drift of the Pound-Drever-Hall error signal with a wedged electro-optical crystal for squeezed state generation," Opt. Lett. **41**, 3331–3334 (2016).
[48]Z. X. Li, Y. H. Tian, Y. J. Wang, W. G. Ma, and Y. H. Zheng, "Residual amplitude modulation and its mitigation in wedged electro-optic modulator," Opt. Express **27**, 7064–7071 (2019).